REPORT DOCUMENTATION PAGE

The public reporting burden for this collection of information is estimated to average 1 hour per response, including the time for reviewing instructions, searching existing data sources, gathering and maintaining the data needed, and completing and reviewing the collection of information. Send comments regarding this burden estimate or any other aspect of this collection of information, including suggestions for reducing the burden, to Department of Defense, Washington Headquarters Services, Directorate for Information Operations and Reports (0704-0188), 1215 Jefferson Davis Highway, Suite 1204, Arlington, VA 22202-4302. Respondents should be aware that notwithstanding any other provision of law, no person shall be subject to any penalty for failing to comply with a collection of information if it does not display a currently valid OMB control number.
PLEASE DO NOT RETURN YOUR FORM TO THE ABOVE ADDRESS.

1. REPORT DATE *(DD-MM-YYYY)* 02-Dec-2009	**2. REPORT TYPE** Final Report	**3. DATES COVERED** *(From - To)* June 17,2009 - September 30, 2009

4. TITLE AND SUBTITLE

An exploration and optimization of the metal insulator transition in vanadium dioxide thin films

5a. CONTRACT NUMBER

5b. GRANT NUMBER
W911NF-08-1-0283

5c. PROGRAM ELEMENT NUMBER

6. AUTHOR(S)
Stuart Wolf

5d. PROJECT NUMBER

5e. TASK NUMBER

5f. WORK UNIT NUMBER

7. PERFORMING ORGANIZATION NAME(S) AND ADDRESS(ES)

University of Virginia
Dept. of Physics
116 Engineer's Way, PO Box 700745
Charlottesville, VA 22904-4714

8. PERFORMING ORGANIZATION REPORT NUMBER

9. SPONSORING/MONITORING AGENCY NAME(S) AND ADDRESS(ES)

U.S. Army Research Office
P.O. Box 12211
Research Triangle Park, N.C. 27709-2211

10. SPONSOR/MONITOR'S ACRONYM(S)
ARO

11. SPONSOR/MONITOR'S REPORT NUMBER(S)
54750-PH-DRP

12. DISTRIBUTION/AVAILABILITY STATEMENT

Approved for public release; Distribution Unlimited

13. SUPPLEMENTARY NOTES

14. ABSTRACT

See attached

15. SUBJECT TERMS

16. SECURITY CLASSIFICATION OF:			**17. LIMITATION OF ABSTRACT**	**18. NUMBER OF PAGES**	**19a. NAME OF RESPONSIBLE PERSON** Stuard Wolf
a. REPORT	**b. ABSTRACT**	**c. THIS PAGE**	SAR	9	**19b. TELEPHONE NUMBER** *(Include area code)* 434-243-2402
U	U	U			

Reset

Standard Form 298 (Rev. 8/98)
Prescribed by ANSI Std. Z39.18

An exploration and optimization of the metal insulator transition in vanadium dioxide thin films

Principal Investigator: **Stuart A. Wolf**
Department of Materials Science and Engineering, University of Virginia

I. Executive summary

Vanadium dioxide (VO_2) is an archetypal strongly correlated oxide and could offer many opportunities for new paradigms of information processing, memory and sensing technology based on a phase transition that could be induced by many means. In this project, we developed a better experimental understanding of the metal-insulator transition in VO_2 and explored the various ways to control the transition temperature and hysteresis. Beyond attempts to understand the strong correlation phenomena in VO_2, we hope to demonstrate a phase transition switch based on the electrically induced metal-insulator transition and compare the performance to the state-of-art Si CMOS.

We have examined the influence of intrinsic and extrinsic factors and are still characterizing their impact on the phase transition of VO_2. Nonetheless, we have observed a number of new phenomena during this seed project that will be summarized here. These new phenomena are not only fascinating by themselves but also promise new opportunities in device applications.

(i) Film strain
We demonstrated that the phase transition temperature was very sensitive to the strain state in VO_2 thin films, especially the c-axis length of rutile VO_2. The transition temperature could be shifted from 300 K to 360 K depending on the type and magnitude of film strain along the c-axis. We are the first to discover a unusually large conductance anisotropy in strained VO_2 films and in the case with the largest anisotropy in the insulating state, the anisotropy disappeared above the phase transition temperature. The mechanism of this disappearance remains unclear at this stage. We suspect that the interface between the film and substrate may play an important role in this disappearance. Further TEM and x-ray studies needs to be carried out.

(ii) Transition metal doping
We have attempted to add a small amount of transition metals such as Mn and Cr into VO_2 thin films and observed that we could modify the phase transition. 20 at % Cr doping suppressed the metal-insulator transition in VO_2 below 100 K and introduced strong ferromagnetism with a Curie temperature well above RT. We have used TEM and x-ray absorption spectrum to examine the changes in the microstructure and electronic structure.

(iii) Relaxation dynamics of metal-insulator transition
We attempted to find out the cause of hysteresis and transition width in the metal-insulator transition of VO_2 by examining the relaxation dynamics of such a transition. We have successfully observed this relaxation process and found for the first time that it evolves as the logarithm of time rather than exponentially. This is very unusual and not at all understood!. We believe that further study can elucidate the reasons for the width and hysteresis in the transition and possibly lead to means to control them for various applications.

(iv) Amorphous VO_2 junctions
Along with the effort in preparing high quality VO_2 thin films we are also developing lateral $V/VO_2/V$ junctions by selective anodization. The temperature dependence of the resistance of

these junctions at very low current is very similar to the temperature dependence of the resistance of VO₂ films that exhibit the semiconductor-metal transition but with a smaller resistance change than the pure oxide films. This composite microstructure has been confirmed by the cross-section TEM. Preliminary measurements indicate a very strong non-linear behavior of the current voltage characteristic in which the resistance of the junction changes nearly two orders of magnitude at 300K.

II. Publications:

1. J. H. Claassen, J. W. Lu, K. G. West and S.A. Wolf, *Relaxation dynamics of the metal-semiconductor transition in VO₂ thin films*, in preparation
2. W. Fan, D. Kirkwood, J.W. Lu and S. A. Wolf, *Properties of vanadium and tantalum granular oxide-metal tunnel junctions fabricated by electrochemical anodization*, Applied Physics Letter, **Accepted**
3. W. Yin, K. G. West, J. W. Lu, Y. Pei, S. A. Wolf, P. Reinke, and Y. Sun, *The metal-insulator transition in vanadium dioxide: A view at bulk and surface contributions for thin films and the effect of annealing*, Journal of Applied Physics, 105, 114322 (**2009**).
4. J.W. Lu, K. G. West and S. A. Wolf, *Very large anisotropy in the dc conductivity of epitaxial VO₂ thin films grown on (011) rutile TiO₂ substrates*, Applied Physics Letters 93, 262107 (**2008**)
5. K. G. West, J.W. Lu, L. He, D. M. Kirkwood, W. Chen, T. P. Adl, M. S. Osofsky, S. B. Qadri, R. Hull and S. A. Wolf, *Ferromagnetism in Rutile Structure Cr Doped VO₂ Thin Films Prepared by Reactive-Bias Target Ion Beam Deposition*, Journal of Superconductivity and Novel Magnetism (**2008**)

III. Progress Statement

(i) Metal-insulator transition temperature vs. Strain

We have investigated the influence of epitaxial strain on the metal-insulator transition temperature of VO₂ thin films. We deposited ~ 40 nm VO₂ films on single crystal TiO₂ substrates with various orientations concurrently. A single crystal c-plane sapphire substrate was also included as the reference sample. All samples were deposited concurrently to ensure the identical chemical defects and oxygen vacancies that could be ruled out as the causes as to any difference observed in these films. XRD was used to determine the film orientation and epitaxial strains along c-axis of rutile VO₂.
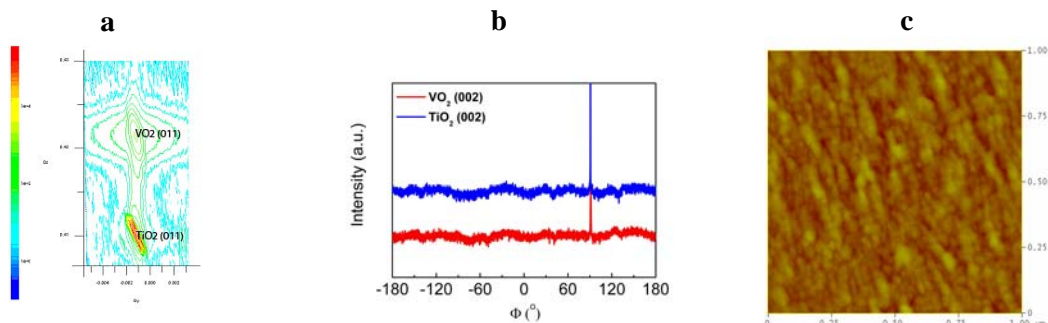

Figure 1 (a) Reciprocal lattice mapping of (011) TiO₂ and (011) VO₂; (b) Phi scan of (002) TiO₂ and (002) VO₂; (c) Atomic force microscope image of (011) VO₂ surface. The RMS roughness is ~ 0.93 nm. VO₂ films were highly epitaxial grown on TiO₂ substrates and had very smooth surfaces.

VO₂ grew epitaxially on TiO₂ substrates despite the large lattice mismatch between VO₂ and TiO₂. Figure 1 shows an example of VO₂ thin film deposited on (011) TiO₂ single crystal substrate. The reciprocal lattice mapping (*Fig. 1a*) showed that the (011) peak in the VO₂ diffraction was closely coupled to that of rutile TiO₂. Only the VO₂ (011) peak along with the TiO₂ (011) peak was detected in 2theta scans, indicating that the film was free of other phases of vanadium oxides. The phi scan of the (002) peak of VO₂ and TiO₂ again confirmed the epitaxy of the VO₂ film (*Fig. 1b*). *Fig. 1c* is an AFM image of (011) VO₂ film surface over an area of 1 μm². The film surface was remarkably smooth with the root-mean-square (RMS) roughness of ~ 0.92 nm. There were no pin holes or nano cracks observed, thus the influence of these defects on the transport properties can be ruled out.

Table 1 Strain and transition temperature of VO₂ films vs. the TiO₂ substrate orientation.

| TiO₂ orientation	Strain along c-axis of rutile VO₂ (%)	T_{MIT} (K)
100	4.79	~340
001	-0.63	293
110	3.47	331
011	-0.42	310
* sapphire		325

VO₂ showed tetragonal symmetry in the phi scan, which was likely due to the substrate clamping effect. Therefore we will only use the notation of rutile VO₂ in the following discussion. The lattice constants, especially the c axis spacing, were calculated from the in-plane and out-of-plane 2theta scans. The strains along the c-axis as a function of the substrate orientation are summarized in *Table. 1*.
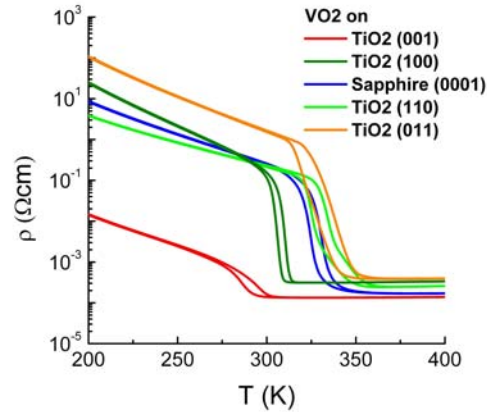
Figure 2 Resistivity vs. temperature for 40 nm thick VO₂ films grown on various substrates.

Figure 2 shows the metal-insulator transition temperature of VO₂ thin films deposited on different substrates. The reference sample deposited on sapphire didn't undergo significant strain due to the lack of in-plane epitaxy and it showed a transition temperature of 325 K. On the TiO₂ substrates, VO₂ films showed an epitaxial relationship. Due to the epitaxial strain, the metal-semiconductor transition temperature was shifted depending on the strain type and magnitude (listed in *Table 1*). The large tensile strain along the c-axis of rutile VO₂ increased the transition temperature. For example, the transition temperature of VO₂ grown on (100) TiO₂ is 340K that was almost 15K higher compared to that of the reference sample. In contrast, the compressive

strain in the sample grown on (001) TiO$_2$ shifted the transition below room temperature (~293 K). It was indicative that the transition as well as the resistivity of VO$_2$ was very sensitive to the strain state that could potentially provide us a new mechanical means to engineer and control the metal-insulator transition of VO$_2$.
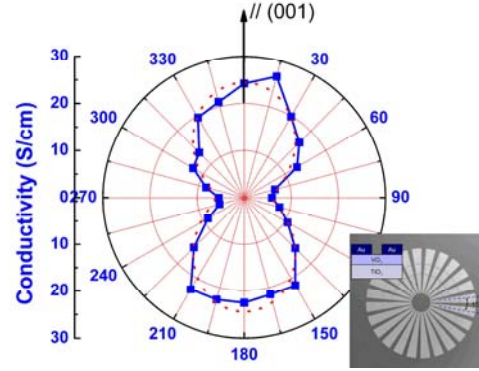

Figure 3 Angular dependence of the conductivity of a VO$_2$ film grown on a (011) TiO$_2$ substrate. The inset was a photograph of Au top contacts and the schematic of the structure.

We realized that the high quality epitaxial films provided a vantage point to inspect the conductance anisotropy of VO$_2$ under strain and found that the film strain also played an important role in the conductance anisotropy of VO$_2$. We designed a circular pattern that could allow us to measure the dc conductivity as a function of in-plane angle. *Fig. 3* shows such measurement result of VO$_2$ grown on a (011) TiO$_2$ substrate. With the assist of the in-plane XRD phi scan, we translated the in-plane directions to the crystallographic orientations of the epitaxial VO$_2$ film. The maximum conductivity (σ_{max}) was 24.21 S·cm, which was parallel to the c-axis of the rutile VO$_2$. In comparison, the minimum conductivity (σ_{min}) was 5.41 S·cm and it occurred perpendicular to the c-axis of rutile VO$_2$. Therefore, the anisotropy ratio, $\frac{\sigma_{max}}{\sigma_{min}}$, was ~4.5 in the (011) plane. We calculated σ_1 (conductivity along (100) and (010) crystal direction) and σ_3 (conductivity along (001) crystal direction) were 6.16 S·cm and 31.64 S·cm respectively. Thus the anisotropy ratio ($\frac{\sigma_3}{\sigma_1}$) was ~5.14 which was much larger than that of a single crystal VO$_2$ (~2).

Fig. 4 shows the conductivity of the (011) VO$_2$ film as a function of temperature along two different directions. Below the transition temperature, the resistivity behaved as a typical variable range hopping conduction that was observed in VO$_2$ and Cr doped VO$_2$ films. The anisotropy ratio was slightly increased at lower temperatures. Strikingly, the anisotropy almost disappeared above room temperature. In contrast, single crystal VO$_2$ still showed an anisotropic conductivity above the transition temperature and $\frac{\sigma_3}{\sigma_1}$ was slightly increased to ~2.5 above the phase transition temperature. Though further investigation is underway, we suspect that the disappearance of the conductivity anisotropy is likely do to the fact that that the interface becomes more conductive above the phase transition temperature. Consequently, if the behavior above the transition is dominated by the interface conductivity then it is likely that the interface conductivity is not anisotropic in nature. Nevertheless, to determine whether the disappearance of anisotropy is due

to the interface and can be associated with the metal insulator transition, it is necessary to study the transport properties as a function of film thickness of VO_2 in the future.
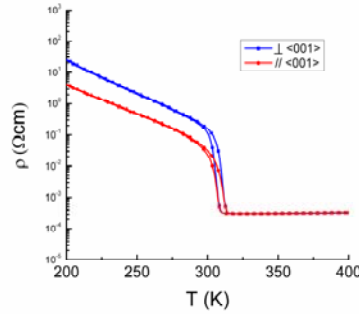
Figure 4 dc resistivity as function of temperature of a VO_2 film grown on a (011) TiO_2 substrate measured parallel and perpendicular to the c axis of rutile VO_2 respectively. The anisotropy ratio was ~ 4.5 below the transition and ~1 above the transition temperature. It was unclear how the anisotropy disappeared in the tetragonal phase and it was not consistent with the observation in VO_2 single crystal.

(ii) Influence of transition metal doping
Our reactive bias target ion beam deposition system (RBTIBD) possesses the capability of growing epitaxial VO_2 with the ability to provide precise doping of transition metals. In the literature, it has been reported that minute amounts of Cr substitution as well as uniaxial stress applied to pure VO_2 leads to a novel phase, *M2*, in which only half of the vanadium atoms dimerize while the other half form spin ½ chains. We have some results on introducing transition metals into VO_2 and studying their influence on the phase transition. Another very intriguing aspect is to determine if we can, by proper doping, engineer a material that undergoes a magnetic transition coincident with the structural or electronic one.

We have successfully introduced 10~20 at % Cr into VO_2 by RBTIBD. X-ray diffraction (XRD) showed that the 10 and 20 at.% $Cr_xV_{1-x}O_2$ films had the tetragonal VO2 structure with lattice constants of 2.270 Å and 2.273 Å respectively. The rutile (020) VO_2 peaks are sharp with FWHM values of $2\theta = 0.19$ degrees and 0.20 degrees respectively, indicating the high quality crystallinity of the material. A clear shift in the peaks to lower angles is observed with increasing Cr concentration indicating an increase in lattice constant. This behavior is not completely understood since the Cr ions were smaller than the V ions. No secondary chromium oxide phases were detected in the x-ray diffraction analysis. The surface morphology was characterized by Atomic Force Microscopy (AFM) that indicated very smooth films having a root-mean-square (RMS) roughness of 3.0 Å over a 5×5 μm^2 scan area. One plausible explanation for the smoothness of our films is growth chamber configuration, and its use of low energy ion beam assisted growth, which has already been demonstrated to smooth metal and oxide thin films during processing.

Fig. 5 shows the resistance as a function of temperature for a pure VO_2 film and a $Cr_{0.2}V_{0.8}O_2$ film, respectively. The pure VO_2 thin film had resistivity of 3.4×10^{-4} Ωcm at 380 K and then underwent an abrupt change of 10^3 in resistivity at its MIT temperature of 341 K. Below the phase transition, the resistivity increased several orders of magnitude to 1.7×10^3 Ωcm at 100 K, which followed a typical variable-range-hopping conduction temperature dependence. The $Cr_{0.2}V_{0.8}O_2$ film has resistivity of 1.4×10^{-3} Ωcm at 380 K that was slightly larger than that of pure VO_2 film. However, the abrupt change in the resistivity did not appear down to 100 K. Instead, it only showed a

variable-range-hopping conduction behavior. Below 285 K the experimental data was fitted to a variable-range-hopping conduction mechanism developed by Mott.
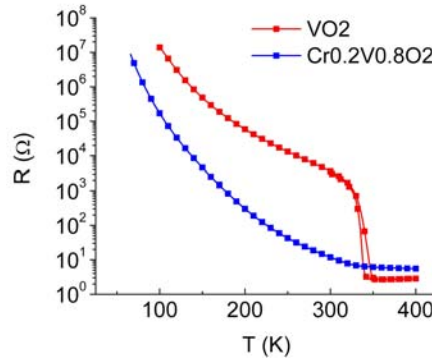
Figure 5 R vs. T for a pure VO$_2$ film and a Cr$_{0.2}$V$_{0.8}$O$_2$ film. Cr$_{0.2}$V$_{0.8}$O$_2$ films was a poorer metal compared to pure VO$_2$ above the transition temperature, but there was no abrupt change in the resistivity that indicated no first order phase transition in Cr$_{0.2}$V$_{0.8}$O$_2$.

In-situ electron diffraction was performed on the 20 at. % Cr doped VO$_2$ thin film taken at 100 and 293 K (*Fig. 6*). We found extra reflections that could be caused by either planar defaults or a long range ordering in the microstructure. Nonetheless the electron diffraction patterns supported the identification of the tetragonal VO$_2$ structure at room temperature that coincided with observations made by XRD experiments. Simulated electron diffraction patterns for the VO$_2$ rutile and monoclinic phases showed the increased asymmetry of the monoclinic phase, which was absent from the experimental pattern. There was no change in the electron diffraction pattern between room temperature and 100 K, suggesting that the structural phase transformation was suppressed at least to temperatures of 100 K.
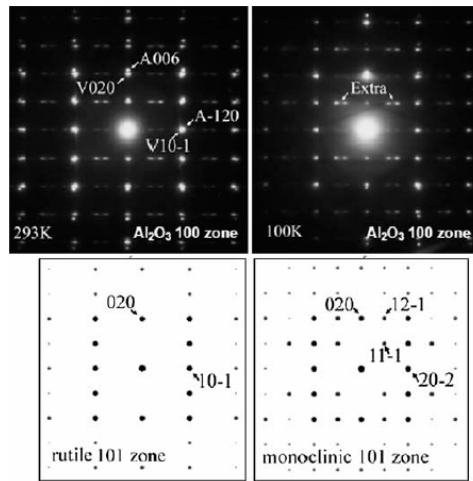
Figure 6 Electron diffraction patterns along the Al$_2$O$_3$ [100] zone taken at 293 K and 100 K and simulated diffraction patterns of the VO2 rutile and monoclinic phases. No extra diffraction spots were observed at 100 K in comparison with that at room temperature that indicated no structural change occurred in this temperature range.

The large amount of Cr doping (20 at.%) had dramatically suppressed the structural phase transition by probably stabilizing the tetragonal structure of VO$_2$ down to cryogenic temperatures. As a result, there is no abrupt change in the resistivity in Cr doped VO$_2$. It is worth noting that CrO$_2$ has a rutile (tetragonal) structure and is a room temperature half metal with 100 % spin

polarization. We have sent $CrVO_2$ for the x-ray spectroscopy (K. Smith, BU) and found out that Cr^{4+} in $CrVO_2$ demonstrated the same electronic structures of half-metallic CrO_2, which explains the room temperature ferromagnetism that we observed in the 20 at. % Cr doped VO_2. They also observed a band gap at room temperature that suggested a semiconducting phase for $CrVO_2$ by comparison with VO_2. The semiconducting phase is consistent with the resistivity measurements of 20% Cr-doped VO_2 shown in *Fig. 5*. As a result, it may indicate a new semiconducting VO_2 phase with the rutile structure (not the monoclinic). These results are implying that the metal-insulator transition in VO_2 might be independent of the structural transition which would imply that we might be able to produce a pure Mott transition.

(iii) Relaxation dynamics of metal-insulator transition

When the metal-insulator transition of VO_2 is monitored as a function of temperature, it frequently displays a substantial hysteresis and transition width (see *Fig. 2*). This is most pronounced in polycrystalline thin films. The hysteresis is usually ascribed to the martensitic nature of the structural transition, where several atoms in a unit cell must move simultaneously to reach a phase of lower free energy. This allows substantial supercooling and superheating. The transition width is probably related to variations among the grains. Within the hysteretic region one would expect that there is a relaxation toward an equilibrium resistance vs. temperature curve. We have observed this process and found for the first time that it evolves as the logarithm of time rather than exponentially. This is unusual but not unique; similar behavior is seen in stress relaxation following plastic deformation, decay of a trapped field in a type II superconductor, and magnetization relaxation and is usually described as "creep".
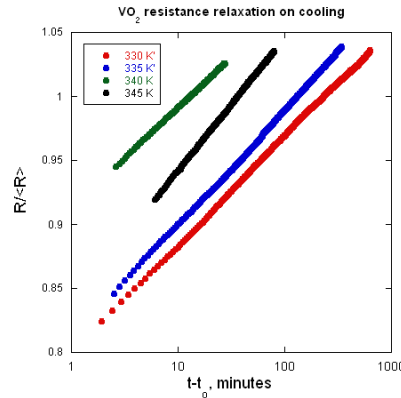

Figure 7 Normalized resistance as a function of time for various temperatures within the transition width. The only fitted parameter is t_o, interpreted as the time the temperature reached the setpoint.

In our experiment we quickly change the temperature of a thin film VO_2 sample from a value well above the metal-insulator transition to a point within the transition. After the temperature has stabilized, we record the resistance as a function of time. The resistance is a measure of the number of crystallites that have transformed from the starting metallic phase to the insulating phase. *Fig. 7* shows that the change in resistance is logarithmic in time. This appears to be independent of which portion of the transition is examined. None of these curves can be fit to an exponential relaxation. We believe that analysis of data like this can elucidate the reasons for the width and hysteresis in the transition and possibly point to means to reduce them.

(iv) Very large non-linear IV in anodized VO$_2$ junctions
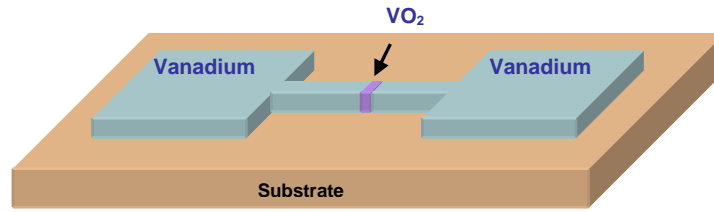
Typical junction dimension: 15 μm×5 μm×0.01 μm

Figure 10 Schematic of a V/VO$_2$/V lateral junction. The VO2 portion was defined by photolithography then anodized to form a nano-composite.

Along with the effort in preparing high quality VO$_2$ thin films we are also developing lateral V/VO$_2$/V junctions by selective anodization following some early and successful work to demonstrate that lateral superconducting tunnel junctions can be made of anodized Nb and NbN thin films. Anodization has been found to be a simple and cost effective technique to produce oxide films of many transition metals. This exploratory work attempts to probe the viability of using anodization as a means of forming a V/VO$_2$/V lateral junction (illustrated in *Fig. 10*). We prepared thin vanadium films, and lithographically defined a narrow stripe and further defined a very short lateral junction region that could be electrochemically oxidized using a novel anodization geometry. In order to investigate the possibility of using electrochemical anodization as a means of producing oxide films for barrier applications several samples of V/SiO$_2$/Si were prepared. An active working electrode area on the pure vanadium films was formed using electroplating tape as a mask and a platinum (Pt) counter electrode was used. Cyclic Voltammetry was performed on an EG&G 273A Potentiostat to determine the activation potential and current density range where the anodization process begins for vanadium. A saturated boric acid (H$_3$BO$_3$) solution with pH adjusted to 7.0 with ammonium hydroxide (NH$_4$OH) was used as the oxygen rich electrolyte. No solution agitation was used for this preliminary study. A fixed DC current of approximately 1 mA/cm^2 was passed through the circuit and the voltage difference across the two electrode setup was monitored. A typical time dependent electric potential (E) observed for this system is shown in *Fig. 11*.
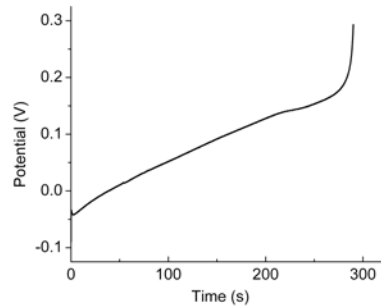
Figure 11 Anodic scan of a 10 nm thick vanadium film. The elbow area in the plot was the region that a composite of metal nano-crystallite and amorphous oxide was obtained.

The temperature dependence of the resistance of these junctions at very low current looked very similar to the temperature dependence of the resistance of VO$_2$ films that exhibit the semiconductor-metal transition but with a smaller resistance change than the pure oxide films (*Fig. 12*). We believe that in the junction region we have a very granular nanostructure of consisting of nanoscale vanadium grains surrounded by a vanadium oxide "nearly amorphous"

matrix whose oxygen stoichiometry and electrical behavior is close to that of the more crystalline VO_2. Thus the short range bonding between the vanadium and oxygen must be similar to that in VO_2, but there is no long range order. This means that this material will be very robust and not subject to degradation due to cycling, either thermal or electrical.
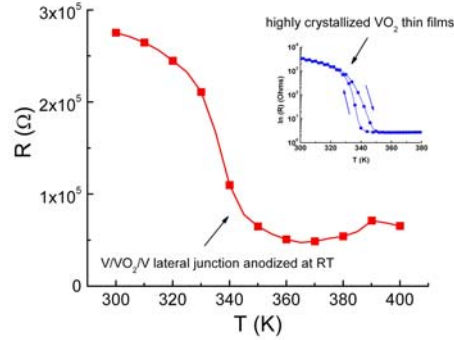

Figure 12 Metal-semiconductor transition of a V/VO$_2$/V lateral junction anodized at room temperature. The inset is the phase transition of VO$_2$ with high crystal quality prepared by Reactive Bias Target Ion Beam Deposition. It is important to point out that the change in resistance has a strong dependence on the measurement current due to the very large non-linear IV behaviors in such junctions.

Preliminary transport measurements indicated a very strong non-linear behavior of the current voltage characteristic in which the resistance of the junction changes nearly two orders of magnitude at 300K at currents between 0 and 0.1 mA (0.1 mA corresponding to a current density of ~6.7×10^4 A/cm^2) (*Fig. 13a*). These unusual non-linear IV curves are shown at 2K, 300K and almost disappearing at 400K where VO_2 becomes metallic. It is also noted a small asymmetry has already been observed and can be seen which may be potential suitable for applications such as diodes. This composite microstructure has been confirmed by the cross-section TEM (*Fig. 13b*).
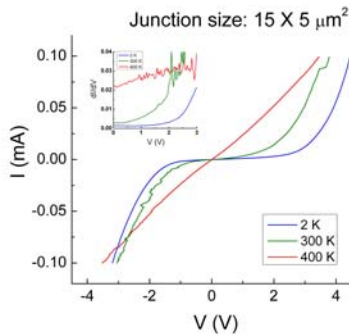
A   B
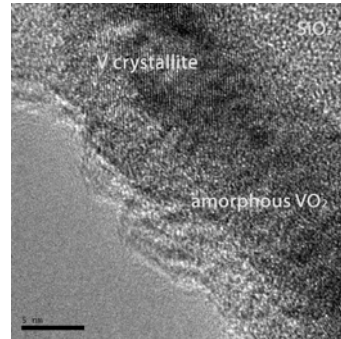
Figure 13 (a) IV curves of V/VO$_2$/V lateral junction. The inset is dI/dVas a function of applied voltage and temperature. It is noticed that dI/dV was highly non-linear from 2 to 300 K that resembled IV behaviors of tunnel junctions and such non-linearity entirely disappeared at 400K; (b) High resolution TEM of anodized VO$_2$ thin films deposited on SiO$_2$. In this image, both ordered area (vanadium crystallites) and non-ordered area (amorphous VO$_2$) coexisted in the anodized regime.